Techno-economic assessment and optimization of a hybrid renewable earth - air heat exchanger coupled with electric boiler, hydrogen, wind and PV configurations

Mohammad Reza Akhtari[1*], Iman Shayegh[1], Nader Karimi[2]

[1]Department of Mechanical and Aerospace Engineering, Shiraz University of Technology, Shiraz 71557-13876, Iran ([*]Corresponding Author: MR.Akhtari@sutech.ac.ir and Akhtari.Reza@gmail.com; I.Shayegh@sutech.ac.ir)

[2]School of Engineering, University of Glasgow, Glasgow G12 8QQ, United Kingdom (Nader.Karimi@glasgow.ac.uk)

Abstract

Energy sectors are responsible for most of greenhouse gas emission in the world. Significant amount of energy is consumed by the residential sector, highlighting the importance of developing sustainable energy technologies for this sector. In the current study, the behavior of an earth - air heat exchanger is simulated numerically, and the results are validated against the existing experimental data. To improve reliability and sustainability, the heat exchanger is coupled with a hybrid renewable energy system, including wind, solar and hydrogen. The performance of this coupled hybrid energy system is explored in continuous and intermittent modes over a period of one month. The results show that nearly half of the drop in total performance of the system occurs during the first working day. Further, running the system intermittently result in an 8% rise in the effectiveness and around 31.55 MJ energy delivery over the period of one month. This implies that

the long-term behavior of the system can be determined by monitoring its behavior on the first day of operation. It is also demonstrated that adding geothermal energy to hybrid renewable energy system can lead to an improvement of about 5.5% of the renewable fraction and decrease emissions and diesel consumption by almost 48%.

Keywords: Earth-air heat exchanger (EAHE); Thermal soil saturation; Renewable Energy; Geothermal energy; Hybrid renewable energy system (HRES)

Nomenclature			
A	cross-sectional area of a pipe (m^2)	n	specific day from January 1st
A_0	amplitude of air temperature (k)	n_0	number of the coldest day
AC	alternating current	NPC	net present cost ($)
ACC	annualized capital cost ($/yr)	NREL	national renewable energy laboratory
ACH	air exchanges per hour (m^3/h)	NTU	number of transfer units
AGC	annual net grid charge ($/yr)	Nu	Nusselt number
AMC	annual maintenance cost ($/yr)	P_r	Prandtl number
ARC	annual replacement cost ($/yr)	PV	photovoltaic
ASE	annual supplied electricity (kWh)	q	air flow rate (m^3/h)
BV	buoyancy-driven ventilation	$Q_{trans.}$	amount of transferred heat (kJ)
COE	cost of energy ($/kWh)	r_i	inner radius the pipe (m)
C_p	specific heat at constant pressure (J/kg.K)	r_o	outer radius the pipe (m)
C_R	replacement cost ($/kW)	RF	renewable fraction
DC	direct current	SAM	system advisor model
$EAHE$	earth-air heat exchanger	$T_{\alpha,in}$	inlet air temperature (k)
E_{nonren}	non-renewable electrical production (kWh/year)	t	Pipe thickness (m)
E_{served}	total electrical load served (kWh/yr)	$T_{\alpha,l}$	air temperature through the pipe (k)
f_{ren}	renewable energy factor	$T_{a,out}$	outlet air temperature (k)
GRBM	generalized RBM model	t_R	time during project lifetime
H	convective heat transfer	$T_{s,z}$	soil temperature at the depth of z (k)
H_{nonren}	nonrenewable thermal production (kWh/year)	T_{wall}	wall temperature of pipe (k)
HOMER	hybrid optimization model for electric renewable	u	Inlet air velocity (m/s)
HRES	hybrid renewable energy system	U_t	overall heat transfer coefficient (W/m^2k)
H_{served}	total thermal load served (kWh/yr)	V	volume of room (m^3)
Hybrid2	hybrid power system simulation model	z	depth of soil (m)
IEA	international energy agency	α	heat penetration coefficient of soil (W/m^2k)
iHOGA	improved hybrid optimization by genetic algorithms	δ	soil layer thickness (m)
IRR	internal rate of return	ε	rate of heat transfer
k_s	soil thermal conductivity (W/m.K)	Δt	temperature differences between the inlet and outlet air temperature
L	length of buried pipe (m)	Δt_{lm}	logarithmic mean temperature difference
$LCOE$	levelized cost of energy	η_R	times during project lifetime
$\dot{m}$	mass flow rate (kg/s)	ρ	air density (kg/m^3)
		ρ_s	soil density (kg/m^3)

29

1. Introduction

The staggering increasing rate of energy consumption and the subsequent environmental issues have become the greatest concerns of the world [1]. Unfortunately, the largest amount of energy demand continues to be provided by fossil fuels and the resultant global warming makes permanent environmental and socioeconomic damages. It is projected that the world energy consumption will hit the pick of 216.5E+12 MW in 2035 [2]. Thus, it essential to adopt a new policy to encourage using an alternative sources of energy, which are cleaner and renewable, and, more importantly, curb fossil fuels [3]. The thermal energy stored in the earth is a well-established source of renewable energy and there are currently about 1.1 million installations worldwide [4,5]. According to International Energy Agency (IEA) and Fig. 1 [6], geothermal power generation was estimated at about 84.8 TWh, in 2017, and is projected to soar over17 GW by 2023 with the biggest capacity additions predicted in Indonesia, Kenya, Philippines and Turkey. This is while the cumulative capacity reached 14 GW in 2017 and, most importantly, geothermal energy provides 93 thousand jobs opportunities worldwide, approximately 35,000 in the USA and 25,000 jobs around Europe [7].

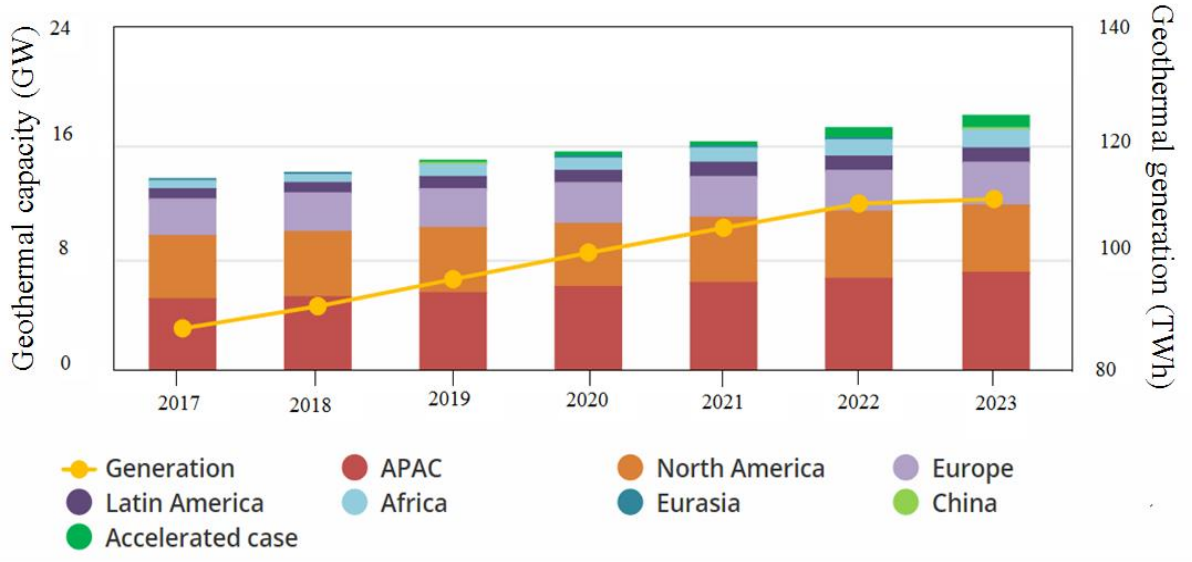

Fig. 1. Geothermal power generation and cumulative capacity by region, 2017-2023 [8].

1.1. Literature review

The temperature of soil oscillate in a shallow layer [9] and remains almost constant in a depth of 2-3 meters or more and is called earth's undisturbed temperature, which is roughly the average of summer and winter temperatures [10,11]. This figure varies with soil moisture, thermal conductivity, location and so on [12]. Chow et al. [13] and Bortoloni et al. [14] explored the ground temperature and found that temperature is sinusoidal throughout the year and depend on the depth. Elminshawy et al. [15] analyzed compactness level of soil on the thermal performance and revealed that the soil compactness of 91.17% could decline air temperature by 21°C.

There are various methods to harness ground thermal energy, among which earth-air heat exchanger (EAHE) has received considerable attention due to its simplicity and low cost [16]. On account of consuming of about 40% of total energy in building section [17,18], EAHE has been

more prevalent and can be seen in private and public constructions [19]. In experimental research of Trombe et al. [20], they investigated using buried pipes in order to chill a hospital naturally. In 1992, Tzaferis et al. [21] compared their analyses with eight methods to evaluate the efficiency of proposed EAHE. Santamouris et al. [22] defined the impact of length, radius, velocity and depth of pipe as well as air velocity through it on greenhouse's efficiency. In another study by Ghosal et al. [23], the performance of a greenhouse over a year was reported while using EAHE. They depicted that the average temperature of greenhouse is about 6-7 $^{\circ}$C lower and 3-4 $^{\circ}$C higher in winter and summer respectively, a higher increase in supplied air, about 12 $^{\circ}$C, has been seen [24,25] and, interestingly, an increment of 16°C was reported in Germany [26]. Besides, Chel and Tiwari [27] simulated vault roof building integrated with EAHE and found that there was an approximately 5 and 15°C difference in inside and outside air temperate in summer and winter respectively, and can be higher in the lower ambient air temperature [28]. Further, pre-heating and pre-cooling were explored in winter and summer in Europe for ventilation goals [29].

Considering soil features, Xinguo et al. [30] investigated the effects of moisture and thermal properties of soil upon the system. Balghouthi et al. [31] focused on dry and moist soil in different conditions and demonstrated that surface temperature in wetted soil fluctuates more than a dry one. Kumar et al. [32] utilized a genetic algorithm for their design and examined different parameters to calculate outlet air temperature. Their figures revealed that the outlet temperature is highly dependent on the temperature of ambient air and surrounding soil. Cucumo et al. [33] put forward a 1D transient analytical model so as that they could predict the temperature of the adjacent soil. Multi-dimensional models have been developed as well [34]. To decrease the outlet temperature of air in the summer by about 5°C, Xamána et al. [35] applied thermal insulation in the final part of underground channels. Diverse kinds of soil have just 2% impact on thermal

performance if the moisture is at the maximum amount [36]. In one numerical simulation [37], sandy soil was realized to be the best ground cover in Malaysian climate, followed by sandy clay loam, clay, loam and silty clay soil. The effect of combined heat and moisture transfer in Gan [38] article. As it was reported, in a depth of 1.5 m, the seasonally averaged heat transfer was 17% more in sandy soil and 14.5% lower in clay soil than in loamy sand one.

Estimating the temperature of soil in various time and depths, Muehleisen [39] proposed an equation to work out outlet air temperature and the sufficient length to design buried pipe. In this research, the temperature of the pipe assumed to be as high as that of soil. Misra et al. [40] and Bansal et al. [41] introduced a new concept as derating factor (determined by the air temperature drops in transient and steady-state conditions) to compare steady with the transient mode. Their analysis was carried out just in 24 hours after starting the system. Therefore, the productivity of configuration was not investigated over a long time and they found that the thermal performance of EAHE fall gradually if the system runs continuously. Moreover, Goswami and Dhaliwal [42] determined the outlet temperature of air within the first 24 working-hour numerically and validate their data with the experimental results. In an experimental study, Vaz et al. [43] used averaged hourly ambient temperature (sinusoidal function) as an inlet temperature to EAHE. Comprehensive data have been reported about the temperature of the soil, ambient and output. May and February have been implied as the appropriate months to take advantage of EAHE for heating and cooling purposes, respectively.

EAHE can be used in the open and closed-loop configuration. Even though the former one is mainly considered to provide fresh air, especially in spacious buildings (e.g. hospitals, public buildings), the latter has better energy efficiency [44,45]. Thanu et al. [46] introduced the correlations between outlet and inlet air temperature to have high effectiveness in summer by

conducting experimental research. Achieving optimized design, Ozgener et al. [47–50] carried out some research on a closed-loop EAHE. Nonetheless, the use of EAHE systems was not so prevalent among people owning to some initial cost-related problems and in high-density housing area, the cost of land and construction are of great importance to capital cost and find location. The soil type and moisture content, relating to the thermal [51]. Uddin et al. [52] compared life-cycle cost between mild steel and polyvinyl chloride pipe. Combining a closed-loop EAHE with heat pump has been studied in a large number of investigations as well [53–55].

Benhammou et al. [56] combined wind tower and EAHE for passive cooling of building to analyze the thermal performance and illustrated the better performance of the hybrid system than each one alone. Also, the thermal performance of EAHE coupled to RSM (response surface methodology) has been better than individual system [57]. Mathur et al. [58] examined straight and spiral EAHE in Jaipur, India. Cooling and heating potential in summer were 343 and 363 kWh and 405 and 418 kWh in winter for straight and spiral arrangement respectively. In two studies [59,60] authors probed into passive EAHE air conditioning system coupled with solar collector and chimney, which could provide the driving force of flow circulation [61]. It was realized that indoor thermal comfort in an appropriate range. In 2018, Lekhal et al. [62] analyzed the thermal performance of a residential house with a direct solar floor and EAHE.

Ghasemi-Fare et al. [63] found that saturated ground cannot be completely elaborated by conductive heat transfer and the heat transfer through temperature-induced pore fluid should be taken into account in the evaluation of thermal performances. In wet configurations, heat transfer rate per unit surface area was measured to be higher than a dry one and comparing dry with 20% moist system, maximum rise in daily heat transfer rate was reported in April, May and June (22.7%, 23.7% and 24.1% respectively) [64]. Fuxin et al. [65] examined the thermal saturation of

soil and temperature fields around the buried pipe. These authors investigated the recovery of surrounding soil by using the system periodically. However, they did not report the interaction between soil and interior air temperature simultaneously in the long-run. Yang et al. [66] addressed this issue by putting forward an analytical method to evaluate the performance of EAHE system. The system faced a periodically fluctuating ambient and soil temperature and the model considered the oscillation in temperature around the pipe. This accounted for wave transmission from the ground surface and that of pipes and the model predicted 3000W in a summer day.

In a numeric study using ANSYS Fluent, Mathur et al. [67] run the system for 12 hours continuously and intermittently, 60 minutes on and 20 minutes off and 60 minutes on and 40 minutes off for 12 hours of working. They also considered different types of soil and found that the intermittent operating system has better performance with a poor thermal conductivity of soil than the continuous mode. Intermittent operating cause the soil temperature and cooling capacity to be recovered among the soil layers by natural heat conduction [68]. In Misra at al. [69] work, the result of continuous (24 hours) and intermittent (three hours on and three hours off periodically) operation in winter revealed that the temperature of soil at the inlet in 0.025 m far from pipe wall fall by 10.1 K, 7.3 K and 5.3 K for thermal conductivity of 4, 2 and 0.52 W/m/K for soil during continuous and 5.6 K, 2.9 K and 1.6 K during intermittent operation, respectively. Stored heat in soil near the pipes can be minimized by using system intermittently and with higher thermal conductivity soil, it could be run continuously, however, the EAHE system must be used in an intermittent mode with lower thermal conductivity soil [70]. There are other investigations on EAHE operating intermittently to assess this method [71,72].

In a recent work, Amanowicz [73] investigated multi-pipe EAHE flow numerically and experimentally to realize the influences of geometry on the pressure losses and flow uniformity.

In this research, 6-36% lower pressure losses were observed in U-type structure than Z-type and coefficients of air flow division uniformity were 11-80% higher. Wei et al. [74] coupled EAHE and buoyancy-driven ventilation (BV) of buildings and developed the first quantitative theoretical model to consider nonlinear coupling effect of the EAHE and BV. Mehdid et al. [75] proposed a new transient semi-analytical model as Generalized RBM model (GRBM) for predicting air temperature through EAHE in continuous behavior. In another study, the EAHE with concrete pipes has been studied in hot-dry weather [76]. Habibi and Hakkaki-Fard [77] evaluated the initial installation cost of four disparate ground heat exchangers: linear, spiral, horizontal and vertical. They showed that for a single arrangement, the linear one has the highest heat exchange rate per pipe unit length, while the spiral configuration has the smallest initial installation expenditure. Generally, altering the center-to-center, pitch and pipe arrangement could make considerable differences in thermal performance [78]. Also, heat exchange rate escalates by having an increment in center-to-center and decrement in pitch.

Supply of energy from completely renewable resources is inevitable in the not-too-distant future and, the demand for such energy is ramping up [79]. More importantly, global warming should be addressed effectively by all nations chiefly by imposing and levying emission taxes to curb the detrimental outcome of fossil fuels [80–82]. This is of vital significance to Iran due to the annual energy consumption of 4.4 times greater than the global average [83]. Iran is located on the world's Sun Belt, with a solar radiation range from 5.4 to 5.5 kW/m^2 per day) and a majority number of sunny days. Iran also has good potentials for generating electricity from wind at about 18,000 MW [84]. This production for wind and solar energy is about 0.5 and 0.1 TWh with annual growth of 10.9% and 119.7%, respectively in 2017 [85].

1.2. Objective

There has been a wide range of studies on geothermal energy and EAHE system, as one of the available technologies to be replaced with those that are based on fossil-fuel. Also, some research has been done to increase the efficiency of the EAHE and provide comprehensive information about the nature of this alternative energy system by coupling it with solar energy. Beyond supplying demands in a stand-alone HRES, the extra generated renewable energy known as excess (or surplus) energy and electricity should be also considered. This is particularly encountered at the peak of renewable energy production in HRES. To increase sustainability and reliability of HRES, this excess electricity should be managed effectively. This can be done through utilization of storage bank to be later used in low-generated energy or high-demand periods, selling to grid or converting to heat in an electric boiler. Moreover, HRES may not be able to meet the demands at peak times or nights when solar radiation is not available. The current work addressed this issue by adding EAHE to HRES. The purpose of this investigation is to analyze a hybrid renewable energy system comprising wind, hydrogen and solar energy to enhance efficiency and reliability of the system and supply the electricity and thermal energy demand to a user. First, the thermal performance of EAHE is analyzed and then the impact of EAHE on hybrid renewable energy system is discussed.

2. Earth - air heat exchanger (EAHE) analysis

In this section we will discuss EAHE in deatails and it will be coupled with HRES in the next section. A numerical method was employed to analyze the problem and generate geometry and mesh, Gambit 2.4.6 (grid generator software) was used and the performance of earth to air heat

196 exchanger system assessed by commercial ANSYS FLUENT 6.3.26, which has been widely used
197 in computational fluid dynamic projects.

198 2.1. Geometry and boundary condition

199 The front side and cross-section view of the simulated domain is demonstrated in Fig. 2,
200 including pipe and nearby soil. In this figure, L, t, r_i and r_o are the length, thickness, inner and outer
201 radius of the pipe, and δ is the thickness of soil. The boundary condition at inlet and outlet is
202 defined as velocity inlet and pressure outlet, respectively. Further, the temperature of the border
203 of the soil domain is considered constant. Thermal and physical properties of soil assumed
204 unchanged over the simulation. No-slip condition with coupled heat transfer is considered on the
205 walls.

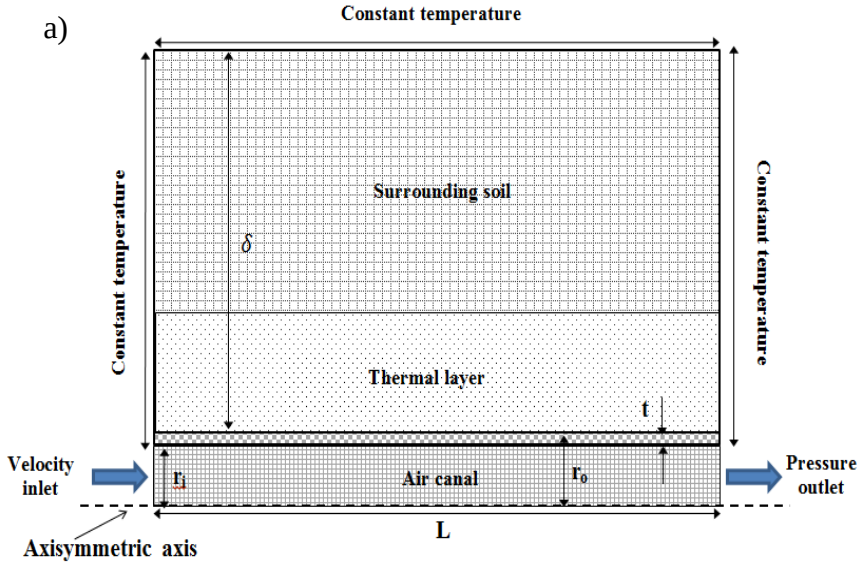

206

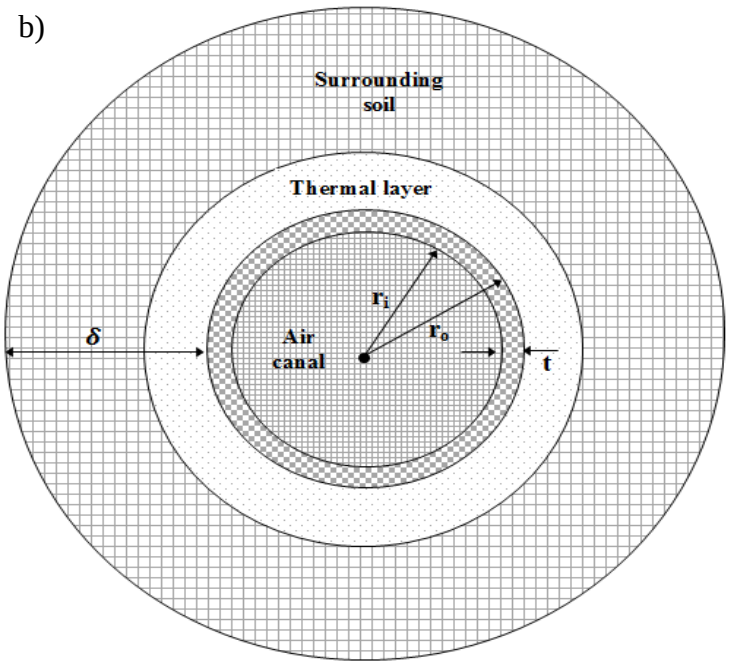

Fig. 2. (a) Front side and (b) cross-section view of the computational domain.

2.2. Model data

For evaluating the problem, the environmental data (such as ambient, soil and inlet air temperature) of Tehran as a city with a moderate climate in Iran is selected. These data are achievable from Mehrabad synoptic station [86] and illustrate that the warmest year happened in 2010. Inlet air temperature was defined as a periodic function with the lowest of 24.2°C and highest of 38°C, which have occurred in June and July in 2010, respectively. The comprehensive information about the EAHE system is provided in Table 1, also applied in the experimental work by Goswami and Dhaliwal [42].

221 **Table 1**

222 Geometric parameters and properties

Parameters	Unit	Value
Pipe		
Length	(m)	25
Diameter	(m)	0.3048
Thickness	(m)	0.002
Buried depth	(m)	2.25
Air		
Inlet velocity	(m/s)	1.475
Specific heat	(J/kg-K)	1205
Thermal conductivity	(W/m-K)	0.028
Density	(kg/m^3)	1.214
Prandtl number		0.77
Soil		
Thermal conductivity	(W/m-K)	1.16
Thermal diffusivity	(m^2/s)	45.6E-7
Buried temperature	(K)	292.039

223

224 2.3. Governing equations

Continuity, momentum and energy equations as well as the k-ε model are employed to carry out the present numerical study [87] in transient mode. Muehleisen [39] estimated the outlet temperature (theoretical method) from ducts by predicting soil temperature in a depth over time.

$$T_{a,L} = T_{s,z} + \left(T_{a,in} - T_{s,z}\right)e^{\left(\frac{-2\pi r_i L U_t}{\dot{m}\, c_p}\right)}, \quad (1)$$

where $T_{a,L}$, $T_{a,in}$, $\dot{m}$ and U_t represent air temperature through the pipe, inlet air temperature, mass flow rate and overall heat transfer coefficient, which can be obtained from the following equation for the pipe with the outer radius of r_o, inner radius of r_i and convective heat transfer coefficient of h between air and inner surface of the pipe.

$$U_t = \left(\frac{1}{h} + \frac{1}{2\pi k_t} Ln \frac{r_o}{r_i}\right)^{-1}. \quad (2)$$

Soil temperature ($T_{s,z}$) can be achieved by the average yearly temperature of ambient air as follow:

$$T_{s,z} = T_m + A_0 e^{\left(-z\sqrt{\frac{\pi}{365\alpha}}\right)} \sin\left(\frac{2\pi(\mathrm{n} - n_0)}{365} - z\sqrt{\frac{\pi}{365\alpha}} - \frac{\pi}{2}\right) \quad (3)$$

In equation (3), T_m is the average yearly temperature of the air, z the depth of soil, n a specific day from January 1st, n_0 number of the coldest day, A_0 amplitude of air temperature (equal to half of the differences between the average temperature of the warmest and coldest months of a year) and α is the heat penetration coefficient of soil and is defined as:

$$\alpha = \frac{86.4k_s}{\rho_s(0.73 + 4.18(\frac{w}{100})} \quad (4)$$

In this equation, k_s, ρ_s and w depict soil thermal conductivity, soil density and soil moisture, which is equivalent to the ratio of water to soil mass.

Paepe and Janssens [88] indicated the effect of various parameters on the thermal and hydraulic performance of EAHE by the 1D theoretical model. In this method, heat loss along pipe and heat transfer between air and pipe wall are calculated via the following:

$$\dot{Q} = \dot{m}c_p\left(T_{a,out} - T_{a,in}\right), \quad (5)$$

$$\dot{Q} = hA\Delta T_{lm}, \quad (6)$$

where ΔT_{lm} is logarithmic mean temperature difference and define as:

$$\Delta T_{lm} = \frac{(T_{a,in} - T_{a,out})}{Ln[(T_{a,in} - T_{wall})\,/(T_{a,out} - T_{wall})]}, \quad (7)$$

in which T_{wall} is the wall temperature of pipe, identical to the soil temperature in buried depth. Thus, the outlet air temperature can be specified by:

$$T_{a,out} = T_{wall} + \left(T_{a,in} - T_{wall}\right)e^{\left(\frac{-2\pi r_i Lh}{\dot{m}\,c_p}\right)}. \quad (8)$$

252 The effectiveness and number of transfer units (NTU), used to calculate the rate of heat transfer in
253 heat exchangers, are as follows.

$$\varepsilon = \frac{T_{a,out} - T_{a,in}}{T_{wall} - T_{a,in}}, \quad (9)$$

254

$$NTU = \frac{hA}{\dot{m}c_p}, \quad (10)$$

255

256 in which, A represents the cross-sectional area of a pipe:

$$A_l = 2\pi r_i L. \quad (11)$$

257

258 Hence, equation (8) can be rewritten as:

$$\varepsilon = 1 - e^{-NTU}. \quad (12)$$

259

260 To compute the heat transfer coefficient the following equation is used:

$$h = \frac{Nuk}{2r_i}, \quad (13)$$

261

262 where the Nusselt number (Nu) is 3.66 when the Reynolds number is less than 2300 otherwise it
263 is obtained from the following relation:

$$\begin{cases} Nu = \dfrac{\xi/8(Re-1000)pr}{1+12.7\sqrt{\left(\frac{\xi}{8}\right)}\,(Pr^{\frac{2}{3}}-1)} \\ 2300 < Re < 10^6, \qquad 0.5 < Pr < 10^6 \end{cases} \tag{14}$$

and

$$\xi = (1.82\ \mathrm{Log\ Re} - 1.64)^{-2}. \tag{15}$$

Inlet air flow rate can be obtained by air change ratio, defined as:

$$\mathrm{ACH} = \frac{3600\dot{m}}{\rho V}, \tag{16}$$

where $\dot{m}$, ρ and V are air mass flow rate, air density and the volume of room, respectively. Therefore, the air flow rate is calculated in m^3/h and by:

$$q = \mathrm{V\ ACH}. \tag{17}$$

Knowing about the volume of target space and its kind, inlet air flow rate is delineated, from which air inlet velocity is calculable:

$$u = \frac{\dot{m}}{\rho A} \tag{18}$$

2.4. Grid study and independence

276 In order to attain independent results from the grid, five different grid networks are considered.
277 As can be seen in Fig. 2, selecting 78,554 computational nodes can be reasonable for the current
278 study. In a fluid zone (air through the canal), a larger number of grids are used than solid zone
279 (soil), where thermal energy conducted among soil layers.

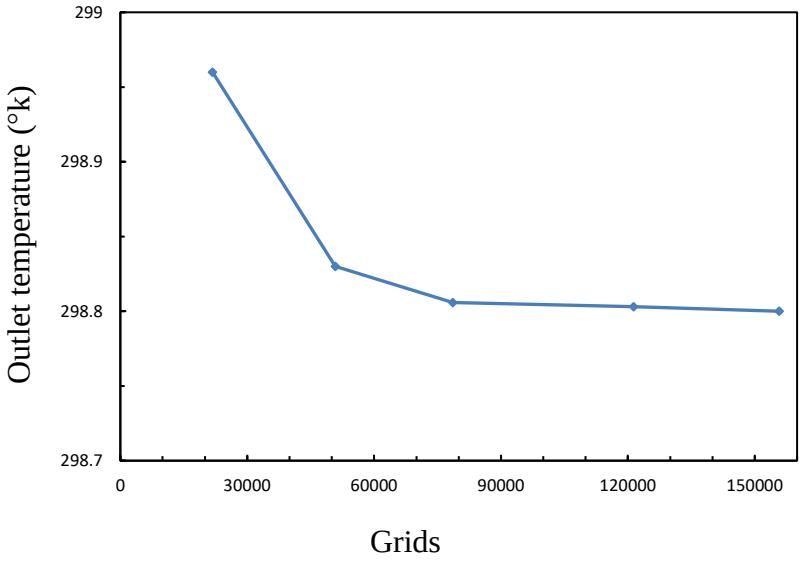

280

281 **Fig. 2.** Outlet air temperature computed by coarse and progressively refined grids.

282

283 Determining optimum time step for transient cases, lead to decreasing simulation time at
284 appropriate cost. The time step independence study is carried out to reach the appropriate one.
285 According to Table 2, by declining time step size less than 10 seconds, the outlet air temperature
286 remains almost constant. Further, the number of iterations for each time step is selected to be 20
287 to have a reasonable computation. The soil thickness around the pipe has been explored and it was
288 realized that considering the thickness of 2 m soil is enough to have the uninterrupted temperature
289 at the frontier of soil boundary conditions.

290 **Table 2**

291 Air temperature at the outlet (time step independence).

Time step (second)	Temperature (K)	Iteration per time step	Temperature (K)
0.5	298.804	10	298.807
5	298.805		
10	298.805	20	298.805
20	298.806	40	298.805
30	298.81		
60	298.82	80	298.804

292

293 2.5. Validation

294 The present numerical study is assessed by comparing with the experimentally generated
295 figures [42] and using data of Table 1. Air temperature through the pipe is depicted 20 and 23
296 hours after running the system in Fig. 3. As can be seen, the present work data and those of
297 experiment are in a good concordance and get better by passing the time. A little variation between

298 the two approaches can be attributed to radiation from the walls and inability to determine the
299 exact properties of soil.

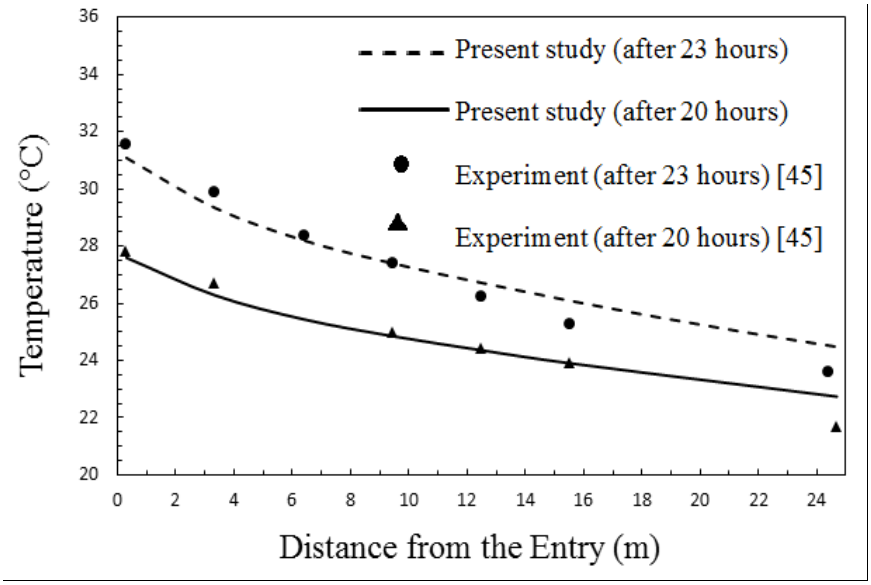

300

301 **Fig. 3.** Comparison of air temperature of the current work and those reported experimentally [42]
302 20 and 23 hours after initiation of the operation.

303

304 2.6. Three-dimensional analysis

305 More accurate result can be gained from 3D simulation in the numerical approach. To verify
306 the acceptability of the current 2D simulation, the air temperature in the pipe has been compared
307 with that predicted by 3D simulations after 23-hour operating. Fig. 4 clearly demonstrates that 2D
308 simulation can be used to minimize the computational time. Besides, the outlet air temperature
309 was compared with the output of TRNSYS (Transient System Simulation Tool), which shows 0.5
310 $^{\circ}$C discrepancy at most, for 30-day running system and admits the output data from ANSYS
311 FLUENT (see Fig. 5).

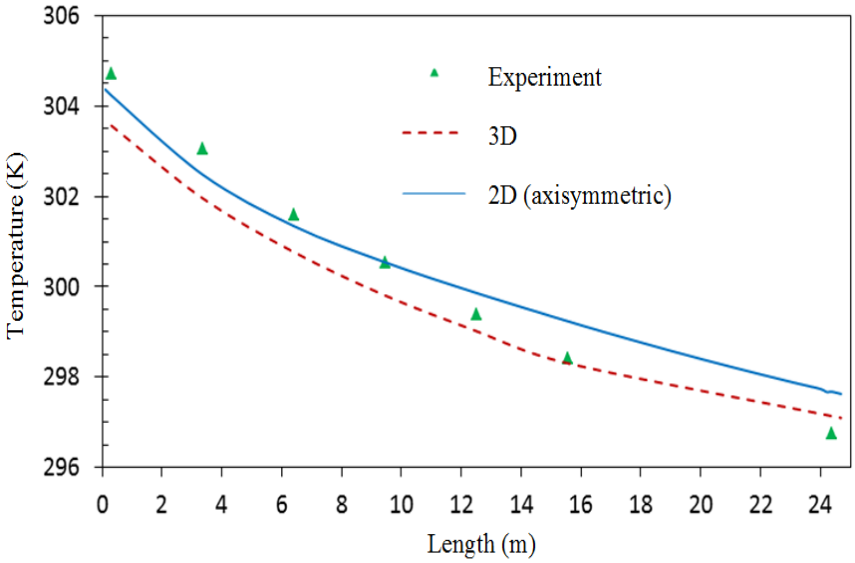

Fig. 4. Air temperature through the pipe, 23 hours after starting the system in 2D, 3D and experimental study.

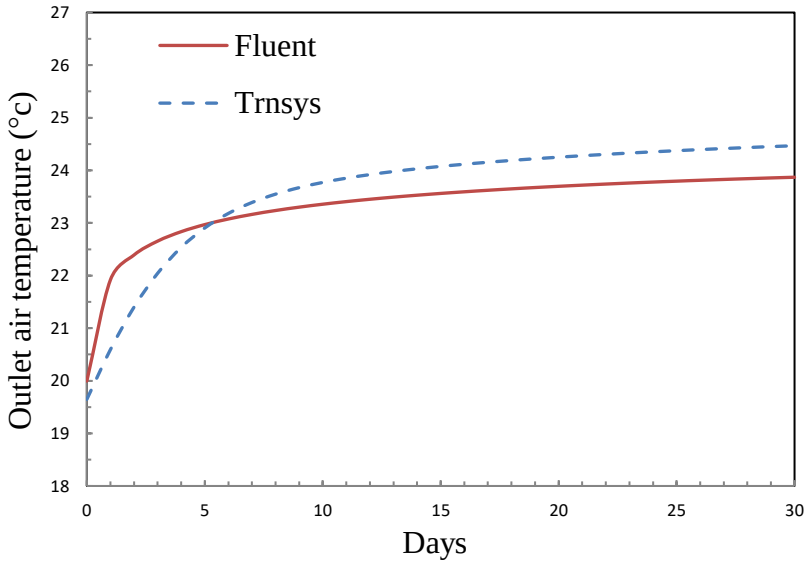

Fig. 5. Comparing outlet temperature predicted by ANSYS Fluent, Trnsys and experiments [42] over the 30-day period.

3. Results and discussion

The air flow rate is defined for 3×4×3 m living room to supply air conditioning. The air exchanges per hour (ACH) is between 3-6 [65,89] and the average value of 4.5 is assumed for the current investigation. Hence, according to equation (17), the rate of 162 m^3/hour air is needed to supply sufficient air, while 306 m^3/hour is required on the basis of cooling load demand [90]. Considering four ducts with 6 inches in diameter and 1.24 m/s (equation 18) inlet air flow can satisfy the ACH and cooling load simultaneously.

3.1. Thermal saturation issue and intermittent operating

As pointed out in the literature, over a period of time, the thermal interactions between the pipe wall and inlet air heat up the surrounding soil and push it to reach its maximum temperature (thermal saturation). Therefore, the intermittent system is adopted to avoid this phenomenon by self-recovery of the system and have better performance in the long-run. To serve this purpose, the EAHE system is switched on from 8 am to 18 pm and is off for the rest of a day while, this pattern occurs every day for purging matter.

Fig. 7 compares the outlet air temperature in continuous with an intermittent mode for the first seven days of operation. The diagram reveals the fact that the differences between the outlet air temperatures of the two systems are maximal in the beginnings hours and this gap narrows reaching the end of the day. The discrepancy between outlet temperatures of the two scenarios after one-hour working is about 0.55°C on the first day and 1.02 and 1.18°C on the subsequent days. This graph clearly illustrates the effect of soil thermal saturation on the outlet air temperature. These data indicate that the greatest impact of self-recovery scenario can be seen on the first day

and the difference between two consecutive days becomes progressively smaller (0.47, 0.16, 0.9, 0.6, 0.4 and 0.3 ˚C respectively for seven successive days of operation).

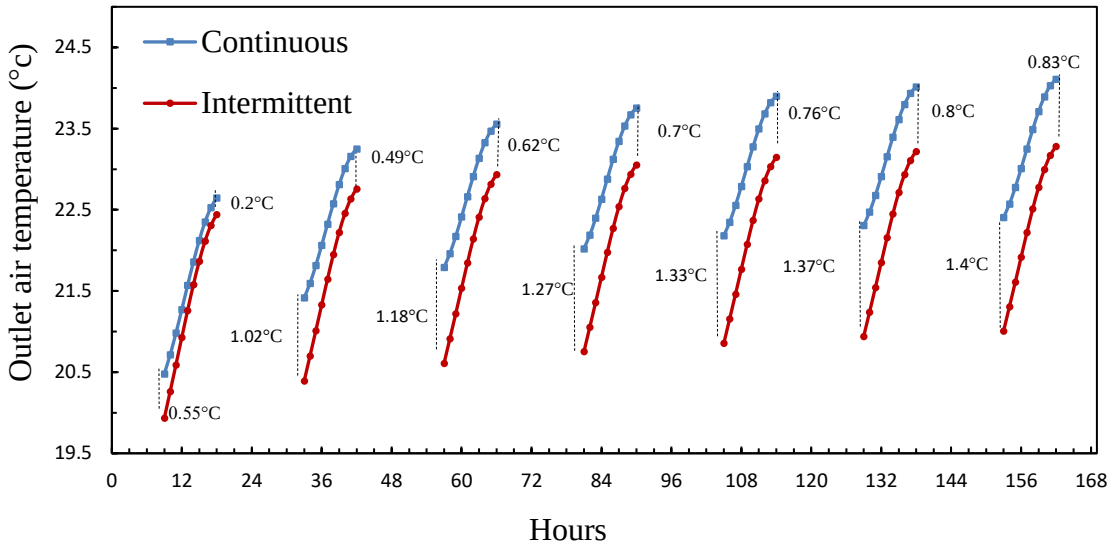

Fig. 6. Comparing the outlet air temperature in continuous and intermittent operation during the first seven days.

As thermal saturation is a transient phenomenon, analysis of EAHE system over a long period is insurmountable to obtain better insight and knowledge. Fig. 7 represents the outlet air temperature over a month. Although the ambient temperature is marginally lower over nights than days and thus imposes less load on the system, switching EAHE off can bring about a desirable effect on the outlet temperature. More interestingly, it can be realized that about 55% of the outlet air temperature decrease occurs overs the first two days (0.69˚C) and, collectively, 1.24˚C decline over a month can be seen by comparing the two modes. Thus, by analyzing the system over the first two days, the response of the intermittent scenario can be understood and estimated over a month. This explains the reason for focus on short-runs in many previous investigations.

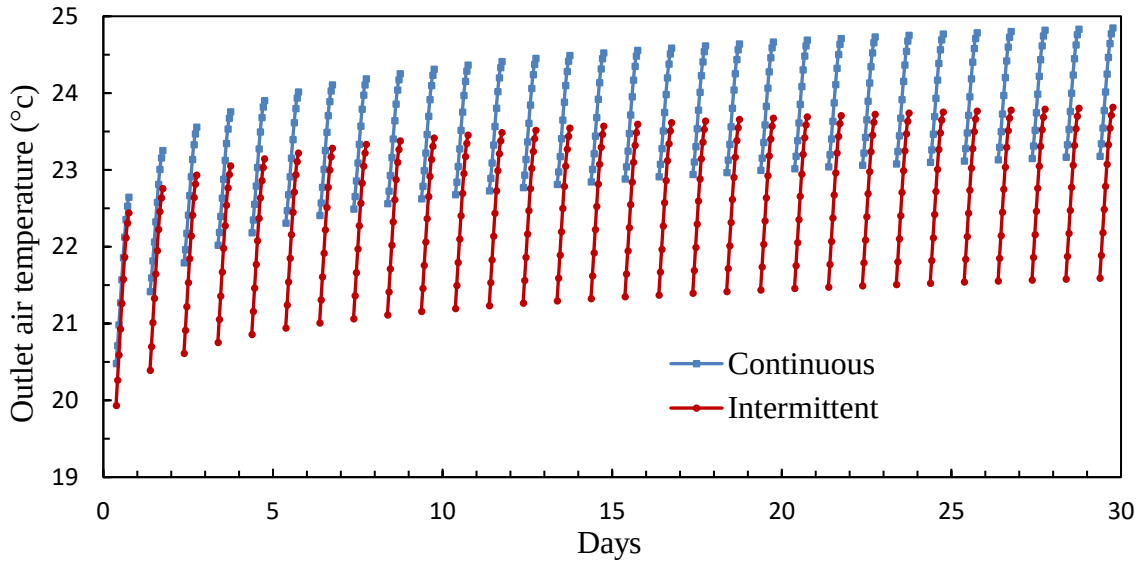

Fig. 7. Comparing the outlet air temperature in continuous and intermittent operation over the first month.

Fig. 8 illustrates the effectiveness of EAHE for a continuous and intermittent system in a period of one month. Approximately 8% increment can be seen when EAHE is operated under intermittent mode over a month. This indicates the superiority of intermittent operation to a continuous one. Besides, this scenario can supply 31.55 MJ heat more than a continuous one at the same time (Fig. 9). This positive point can not only provide better comfort but also contribute to a decrease in greenhouse gas emissions generated by burning fossil fuels.

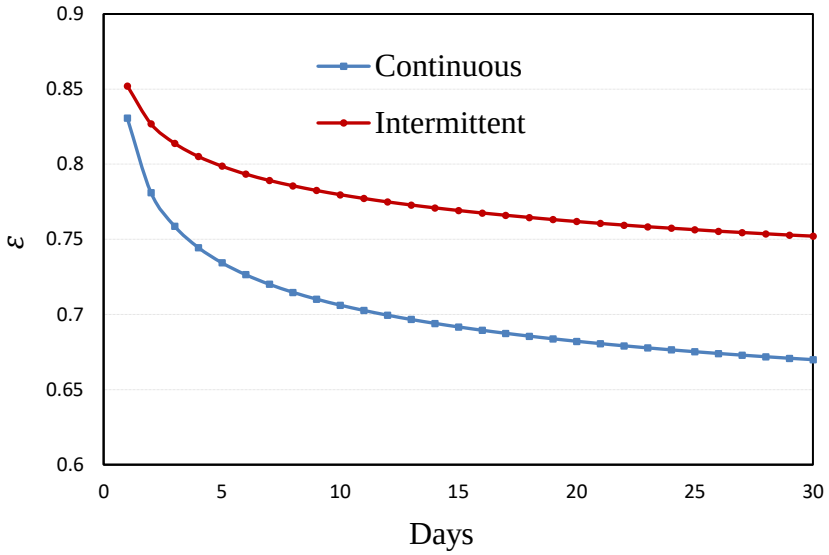

Fig. 8. Comparing the effectiveness of the EAHE system in continuous and intermittent operation over the first month.

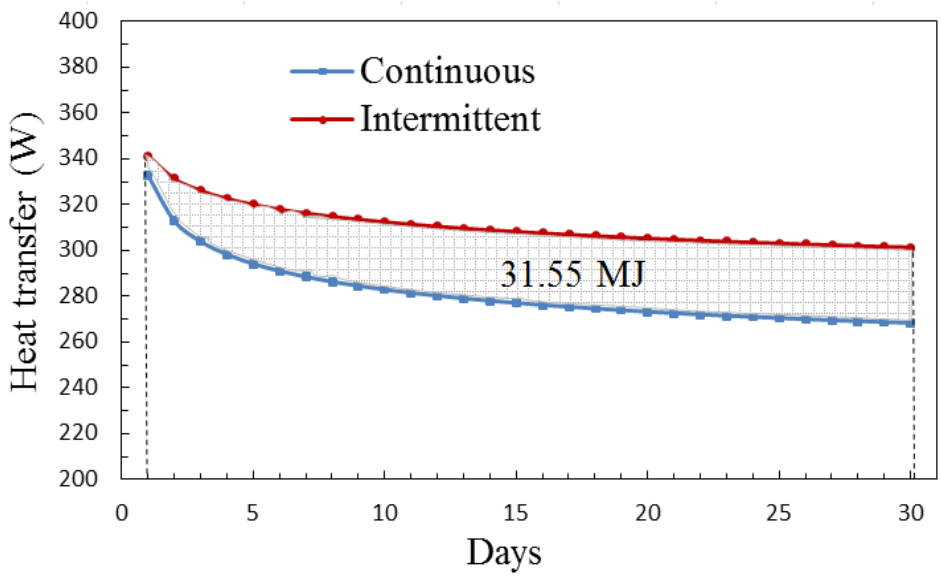

Fig. 9. Comparing the heat transfer of the EAHE system in continuous and intermittent operation over the first month.

4. Hybrid system Wind/PV/EAHE

Generally, HRES includes various available renewable energy components, regarding different situations such as irradiation, wind speed, hydro power, availability, capital and maintenance cost. Considering the suitable irradiation and wind speed in Iran, the proposed HRES includes photovoltaic panels, wind turbine, fuels cell and EAHE. For analysis of hybrid renewable energy systems (HRES), there exists a number of software including RETscreen, HOMER (Hybrid Optimization Model for Electric Renewable), iHOGA (Improved Hybrid Optimization by Genetic Algorithms, Hybrid2 (Hybrid Power System Simulation Model) [91], PVsys, SAM (System Advisor Model). Among these HOMER (an hourly optimization software) is a powerful software developed by NREL (National Renewable Energy Laboratory) [92] and has been used by a variety of scholars worldwide so as to conduct techno-economic analysis and select optimal HRES [93]. In this work, energy balance is adopted for HRES analysis by HOMER on an hourly basis. Energy flow is estimated between generated energy, and thermal and electric load. Further, if the HRES included batteries, it would be decided to charge or discharge the storage banks in each time step. In experimental and numerical studies, HOMER was validated by Shah and Mundada [94] [95] [96]. In the next part of the current work, HRES comprising PV and wind energy is investigated by HOMER then and it will be coupled with EAHE to alleviate the thermal load of a residential building situated in Tehran, Iran. This novel system performs a key role in reducing electricity demand whereby the consumption of fossil fuels can be curtailed and witness emissions decline correspondingly.

4.1. Components and loads

Fig. 10 depicts the general configuration of HRES. Average electricity consumption (according to electricity bill), thermal and hydrogen load demand to supply the energy of residential building are 13.8 kW/day (with a peak of 1.94 kW), 15.7 kW/day (peak 2.64 kW) and 8 kg/day (peak 1.65 kg/hour), respectively. The produced hydrogen from electrolyzer with the pressure of 4 bar can be used in two electric cars, powered by fuel cells, to run about 333 km each day (12g of H_2 per kilometer [97]). All of the surplus of electricity will pass through an electric boiler in HOMER, so there is not any disused electricity, which is a favorable approach to run the HRES. In contrast, the thermal energy may be generated more than what is needed, especially in the afternoon when the PV electricity production is at its highest level. The diesel boiler works only when the electric boiler fails to cover the thermal loads. In such cases, chiefly at nights when the PVs have no production, there is no surplus electricity and the most favorable configuration is achievable.

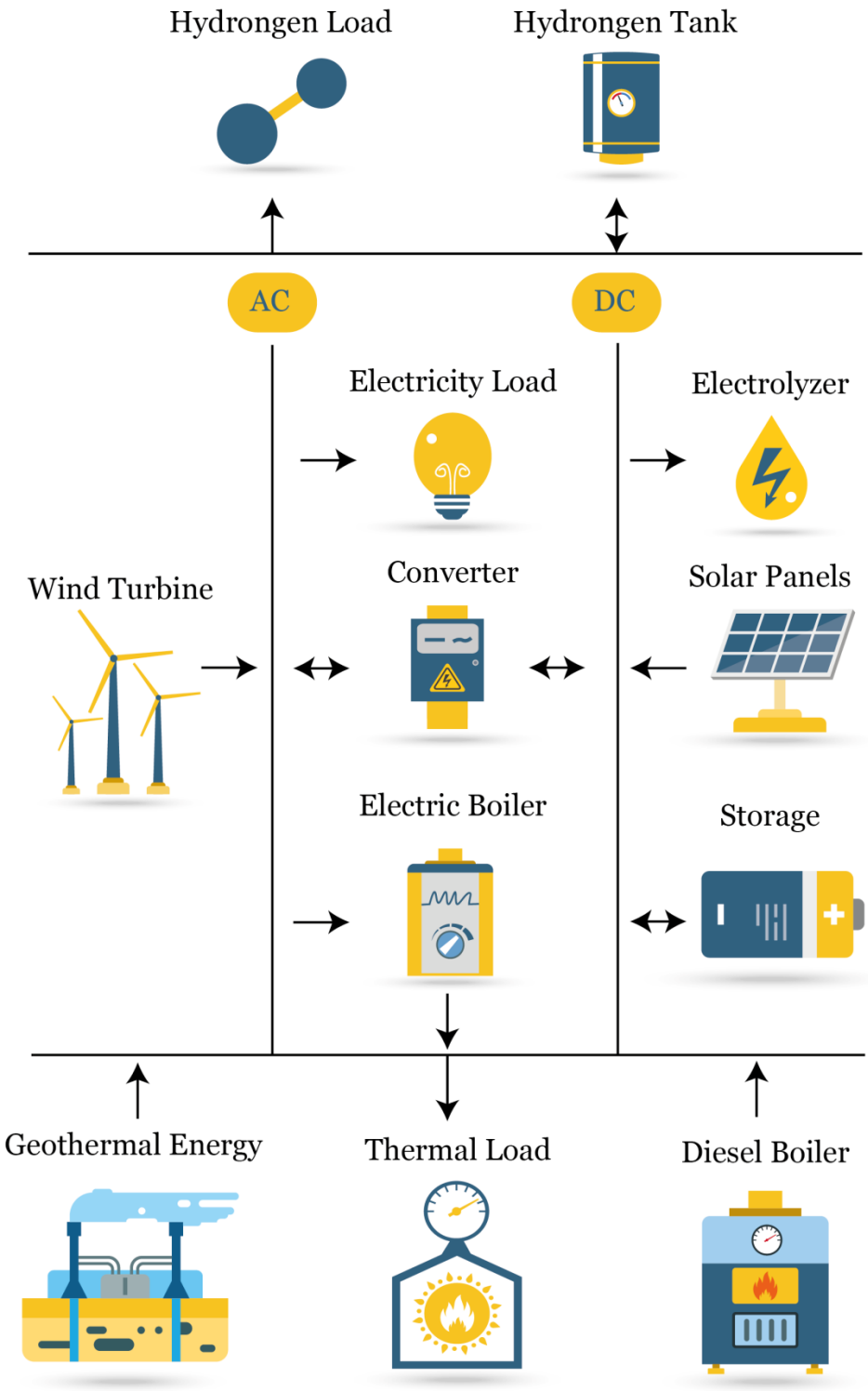

407

408 **Fig. 10.** General configuration of HRES

To select an appropriate wind turbine considering weather condition, various wind turbines with disparate power curves and total capacities are explored. According to Table 3, the Eocycle EO10 with annual electricity production of 17,108 kWh/year, rated capacity of 10 kW, the capacity factor of 19.5 and the cost of energy of 1.7 $/kWh features the greatest economical performance.

Table 3

The levelized cost of diverse wind turbines.

Name	Rated capacity (kW)	Production (kWh/year)	COE ($/kWh)	Capacity factor (%)
aws hc 1.5 Kw	1.5	1,040	7.16	7.91
GENERIC 3 Kw	3	1,102	7.71	4.19
Bergey Excel 6	6	4,293	2.54	8.17
Eocycle EO10	10	17,108	1.7	19.5
Bergey Excel 10-R	10	5,904	2.27	6.74
Bergey Excel 10-R	10	5,859	2.28	6.69
Generic10 kW	10	4,234	2.99	4.83
Xzeres 7.2	10.4	6,587	2.15	7.23
NPS100C-24	95	88,045	4.49	10.6
Leitwind 77 850kW	850	1,049,916	28.24	14.1

Running renewable energy systems is often expensive and, in some cases, HRES performance is highly dependent on weather condition. To analyze the system, technical details (Table 4) and the cost of components are illustrated (Table 5) to calculate COE in HRES and find out the most cost-effective one. Moreover, project lifetime is assumed to be 20 years, inflation rate 2%, diesel price is 1.05 $/l and the interest rate of 7% is considered. HOMER has a rich component library, which has been used for many years by numerous researchers [98,99]; however, each component library

can be accommodated to reach a favorable one. Therefore, extensive data have been used from HOMER library and also the local market information for those devices that HOMER does not offer any technical details. The detailed datasheet is available for Eocycle EO10 wind turbine [100] and CELLCUBE® FB 30-130 battery [101]. Also, the Varmeteknikk AS electric boiler [102,103] is chosen for thermal energy production from surplus electricity.

Table 4

Type and costs of components.

Component	Lifetime	Capital cost	Replacement cost	Operation and maintenance
Flat plate PV	25 years	2000 $/kW	2000 $/kW	10 $/kW/yr
System convert	20 years	300 $/kW	300 $/kW	0 $/kW/yr
Wind turbine	20 years	2000 $/kW	1800 $/kW	500 $/turbine/yr
Electrolyzer	20 years	5000 $/kW	5000 $/kW	0
Hydrogen tank	25 years	574 $/kg	574 $/kg	0 $/kg/yr
Storage battery	20 years or 2628000 kWh	2300 $/kWh	2250 $/kWh	0 $/h
Electric boiler	20 years	54 $/kW	54 $/kW	0 $/kW/yr

Table 5

Technical data of the system.

Component		
Flat plate PV	Nominal operation cell temperature	47 °C
	Temperature coefficient	- 0.5 %/°C
	Efficiency at standard test condition	13%
	Derating factor	80%
System convert	Inverter efficiency	95%
	Rectifier efficiency	95%
	Rectifier capacity	100%
Eocycle EO10 wind turbine	Rated capacity	10 kW
	Rotor diameter (m)	15.8 m
	Tip speed	44 m/s
	Hub height	24 m
	Swept area	196.3 m^2
	Cut-in wind speed	2.5 m/s
	Cut-out wind speed	20 m/s
Generic electrolyzer	Efficiency	85%
	Minimum load ratio	0%
Generic hydrogen tank	Initial tank level	20%

CELLCUBE® FB 30-130 battery	Nominal capacity	130 kWh
		2710 Ah
	Round trip efficiency	64%
	Nominal voltage	48 V
	Max charge current	583 A
	Max discharge current	911 A
Generic electrolyzer	Efficiency	85%
Generic hydrogen tank	Initial tank level	20%
Generic boiler	Efficiency	85%

435

436

437 4.2. Financial issue

438 Petrou [104] raised an interesting issue on the levelized cost of energy (LCOE). It was
439 mentioned that there are some variables that affect the cost of energy (COE) such as the capital,
440 operation and maintenance costs, and the economic lifetime and investment as well. Investment
441 cost including the material, foundation, transporting, assembling, installations, connection to
442 utilities and so on [105]. The local data, HOMER library as well as references for PV [106],
443 electrolyzer [107] and electric boiler [102] are used to obtain optimum system. COE is calculated
444 by [99]:

445

$$COE = \frac{ACC+ARC+AMC+AGC}{ASE}$$
$$COE = \frac{ACC + ARC + AMC + AGC}{ASE} \quad (19)$$

446

447 ASE, AMC and AGC are the annual supplied electricity, maintenance cost and net grid charge.
448 The annualized capital cost (ACC) and replacement cost (ARC) are determined as:

$$ACC = \frac{i(1+i)^N}{(1+i)^N-1} I_{0,}$$
$$ACC = \frac{i(1 + i)^N}{(1 + i)^N - 1} I_{0,} \quad (20)$$

449

$$ARC = \frac{i(1+i)^N}{(1+i)^N-1} \sum_{\eta_R} \frac{C_R}{(1+i)^{t_R}},$$
$$ARC = \frac{i(1 + i)^N}{(1 + i)^N - 1} \sum_{\eta_R} \frac{C_R}{(1 + i)^{t_R}}, \quad (21)$$

450

451 where C_R, t_R and η_R are the replacement cost, time and times during project lifetime, respectively.
452 When NPV is zero, the interest rate will reduce to the internal rate of return (IRR), which is
453 applicable in the evaluation of hybrid system [108]:

$$\sum_{t=1}^{N} \frac{R_t - C_t}{(1+i)^t} = I_0$$
$$\sum_{t=1}^{N} \frac{R_t - C_t}{(1 + i)^t} = I_0 \quad (22)$$

454

The higher the IRR, the more appealing is the project economically for stockholders. Another factor is the net present cost (NPC), which represents the life cycle cost of the system [109]. Costs include capital, replacement, operation and maintenance, fuel costs and emissions penalties. Renewable energy factor can be defined as [110]:

$$f_{ren} = 1 - \frac{E_{nonren} + H_{nonren}}{E_{served} + H_{served}} \tag{23}$$

where E_{nonren} is nonrenewable electrical production (kWh/year), H_{nonren} is nonrenewable thermal production (kWh/year), E_{served} is total electrical load served (kWh/year) and H_{served} is total thermal load served (kWh/year).

4.3. Optimization

The two most optimized systems by HOMER are illustrated in Table 6, which are based on COE and are $ 13.92 and $ 14.28, and renewable fraction (RF) for these two configurations are 84.3 and 86.2, respectively. The calculations in this part are irrespective of EAHE expenditure in the system. In order to diminish surplus of electricity in HRES, electric boiler, which can be defined as thermal load controller (TLC) in HOMER, is used to enhance the renewable fraction of the system and curb fossil fuels consumption correspondingly.

Table 6

Optimized HRES

PV (kW)	WT	Battery (quantity)	Electrolyzer (kW)	Hydrogen tank (kg)	TLC (kW)	Converter (kW)	NPC ($)	Initial cost ($)
221	1	1	65	38	154	8	889,816	888,728
247	0	1	65	38	163	2	913,164	919,414

The most optimum system has been chosen for further analysis. Fig. 11 depicts the amount of electricity production by disparate parts of the HRES. The differences between these two figures are known as excess electricity (or surplus of electricity), which is an issue in HRES. There are numerous methods to curb this undesirable aspect such as selling this extra energy to the grid. This approach not only can help the grid but also can generate revenues and make a profit for the owner. However, it is impossible to access the grid in remote areas. Another possible way is to add a handful of storage systems for peak demand or other purposes, which may impose a further cost on an investor or it may be the case that there is not any other demand. A sensible way of curbing this adverse outcome that is used in the present study is to convert excess (surplus) electricity to another form of energy like thermal one and can be used for heating purposes. As mentioned earlier, it can be achieved by the electric boiler and take a critical step in protecting the environment.

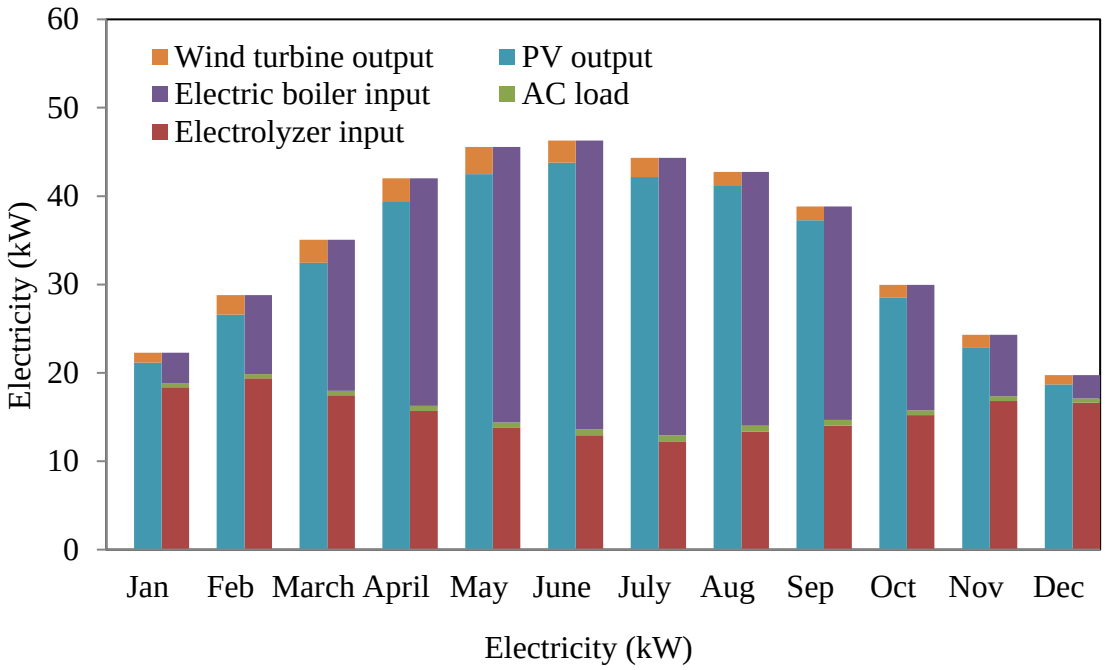

487

488

489 **Fig. 11.** Electricity production and consumption by the optimal configuration.

490

491 By taking the advantage of EAHE, it is possible to supply a certain amount of thermal demand
492 through geothermal energy, which leads to a decrease in diesel consumption by diesel boiler and,
493 more importantly, less emissions through burning fossil fuels. The EAHE, on average, can provide
494 223 kWh, which is about 8.7 kWh more than a continuous one, every month. Hence, it is logical
495 to assume that every year about 2713.2 kWh thermal energy is contributed to HRES by geothermal
496 energy. The amount of transferred heat can be computed by heat exchange equation [111,112]:

$$Q_{trans.} = mC_p\Delta T \qquad (24)$$

497

where m, C_p and ΔT are the mass flow of air (kg), specific heat at constant pressure, which is about 1 kJ/kg-K, and temperature differences between the inlet and outlet air temperature

$$\Delta T = T_i - T_o. \quad (25)$$

By coupling HRES with EAHE, it is possible to restrict emissions and boost renewable energy fraction. According to Table 7, adding EAHE to the current HRES can lead to an about 48% and 49% fall in exhausted CO_2 and diesel consumption respectively, and a 5.5% increase in RF.

Table 7

EAHE impact on emission reduction and RF rise

HRES	Renewable Fraction (%)	Diesel (L/year)	Carbon dioxide (kg/year)	Sulfur dioxide (kg/year)
Without EAHE	84.3	202	535	1.33
EAHE	88.9	103	273	0.68

5. Conclusion

Thermal performance of EAHE was examined under continuous and intermittent (8 am to 18 pm) operational modes. To validate the results, they were compared with the experimental and TRNSYS data. Working periodically aids the configuration to be self-recovered. This phenomenon

demonstrates its soundness in the long-run. The present study revealed that intermittent scenario can improve the effectiveness of the system by about 8% in a month, which is almost 31.55 MJ energy delivery more than the continuous mode. It should be noted that 55% of the outlet air temperature reduction happens during the first two days of working. That is 0.69°C and reaches 1.24°C after one month operating.

Finally, EAHE was coupled with PV, hydrogen and wind energy to enhance renewable energy factor and sustainability of the HRES. Additionally, this new hybrid system can enhance the reliability of the system (geothermal energy is chiefly available everywhere at any time) and cut many kinds of emission from fossil fuels. The effect of EAHE on HRES was investigated and the investigation revealed that HRES+EAHE can enhance the renewable fraction by about 4.5% and decrease the exhausted CO_2 and diesel consumption by approximately 48%. All the same, to enjoy the most cost-effective renewable energy system, extensive studies are vital on this matter, especially using hybrid systems to enhance the sustainability and reliability of energy systems.

References

[1] B.K. Sovacool, S.V. Valentine, M. Jain Bambawale, M.A. Brown, T. de Fátima Cardoso, S. Nurbek, G. Suleimenova, J. Li, Y. Xu, A. Jain, A.F. Alhajji, A. Zubiri, Exploring propositions about perceptions of energy security: An international survey, Environ. Sci. Policy. 16 (2012) 44–64. doi:https://doi.org/10.1016/j.envsci.2011.10.009.

[2] W.H. Azmi, M.Z. Sharif, T.M. Yusof, R. Mamat, A.A.M. Redhwan, Potential of nanorefrigerant and nanolubricant on energy saving in refrigeration system – A review, Renew. Sustain. Energy Rev. 69 (2017) 415–428.

534 doi:https://doi.org/10.1016/j.rser.2016.11.207.

535 [3] M. Mohammadi, Y. Noorollahi, B. Mohammadi-Ivatloo, H. Yousefi, Energy hub: from a
536 model to a concept–a review, Renew. Sustain. Energy Rev. 80 (2017) 1512–1527.

537 [4] J. Lund, B. Sanner, L. Rybach, R. Curtis, G. Hellstrom, Geothermal (ground-source) heat
538 pumps-a world overview, (2004).

539 [5] S. Karytsas, H. Theodoropoulou, Public awareness and willingness to adopt ground source
540 heat pumps for domestic heating and cooling, Renew. Sustain. Energy Rev. 34 (2014) 49–
541 57. doi:https://doi.org/10.1016/j.rser.2014.02.008.

542 [6] IEA, Energy Efficiency 2018. Analysis and Outlooks to 2040., Int. Energy Agency.
543 (2018). https://webstore.iea.org/market-report-series-energy-efficiency-2018.

544 [7] RENEWABLES 2018 GLOBAL STATUS REPORT, (n.d.). http://www.ren21.net/wp-
545 content/uploads/2018/06/17-8652_GSR2018_FullReport_web_-1.pdf.

546 [8] Renewables 2018 Market analysis and forecast from 2018 to 2023, (n.d.).
547 https://www.iea.org/topics/renewables/geothermal/.

548 [9] G. Tsilingiridis, K. Papakostas, Investigating the relationship between air and ground
549 temperature variations in shallow depths in northern Greece, Energy. 73 (2014) 1007–
550 1016.

551 [10] A. Skotnicka-Siepsiak, M. Wesołowski, J. Piechocki, Experimental and Numerical Study
552 of an Earth-to-Air Heat Exchanger in Northeastern Poland., Polish J. Environ. Stud. 27
553 (2018).

554 [11] S.S. Bharadwaj, N.K. Bansal, Temperature distribution inside ground for various surface
555 conditions, Build. Environ. 16 (1981) 183–192.

556 [12] O. Ozgener, L. Ozgener, J.W. Tester, A practical approach to predict soil temperature
557 variations for geothermal (ground) heat exchangers applications, Int. J. Heat Mass Transf.
558 62 (2013) 473–480.

559 [13] T.T. Chow, H. Long, H.Y. Mok, K.W. Li, Estimation of soil temperature profile in Hong
560 Kong from climatic variables, Energy Build. 43 (2011) 3568–3575.
561 doi:https://doi.org/10.1016/j.enbuild.2011.09.026.

562 [14] M. Bortoloni, M. Bottarelli, Y. Su, A study on the effect of ground surface boundary
563 conditions in modelling shallow ground heat exchangers, Appl. Therm. Eng. 111 (2017)
564 1371–1377. doi:https://doi.org/10.1016/j.applthermaleng.2016.05.063.

565 [15] N.A.S. Elminshawy, F.R. Siddiqui, Q.U. Farooq, M.F. Addas, Experimental investigation
566 on the performance of earth-air pipe heat exchanger for different soil compaction levels,
567 Appl. Therm. Eng. 124 (2017) 1319–1327.
568 doi:https://doi.org/10.1016/j.applthermaleng.2017.06.119.

569 [16] F. Niu, Y. Yu, D. Yu, H. Li, Heat and mass transfer performance analysis and cooling
570 capacity prediction of earth to air heat exchanger, Appl. Energy. 137 (2015) 211–221.

571 [17] A. de Jesus Freire, J.L.C. Alexandre, V.B. Silva, N.D. Couto, A. Rouboa, Compact buried
572 pipes system analysis for indoor air conditioning, Appl. Therm. Eng. 51 (2013) 1124–
573 1134.

574 [18] K. Amasyali, N.M. El-Gohary, A review of data-driven building energy consumption

575 prediction studies, Renew. Sustain. Energy Rev. 81 (2018) 1192–1205.
576 doi:https://doi.org/10.1016/j.rser.2017.04.095.

577 [19] M. Schuler, Design for daylighting and energy in Ingolstadt, Adv. Build. Newsl. 23
578 (1999) 18–23.

579 [20] A. Trombe, M. Pettit, B. Bourret, Air cooling by earth tube heat exchanger: experimental
580 approach, Renew. Energy. 1 (1991) 699–707.

581 [21] A. Tzaferis, D. Liparakis, M. Santamouris, A. Argiriou, Analysis of the accuracy and
582 sensitivity of eight models to predict the performance of earth-to-air heat exchangers,
583 Energy Build. 18 (1992) 35–43.

584 [22] M. Santamouris, G. Mihalakakou, C.A. Balaras, J.O. Lewis, M. Vallindras, A. Argiriou,
585 Energy conservation in greenhouses with buried pipes, Energy. 21 (1996) 353–360.

586 [23] M.K. Ghosal, G.N. Tiwari, N.S.L. Srivastava, Thermal modeling of a greenhouse with an
587 integrated earth to air heat exchanger: an experimental validation, Energy Build. 36 (2004)
588 219–227.

589 [24] Y.-C. Jeong, Modeling of a hybrid-ventilated building:" Grong school", (2002).

590 [25] J. Zhang, F. Haghighat, Simulation of earth-to-air heat exchangers in hybrid ventilation
591 systems, in: Ninth Int. IBPSA Conf. Build. Simul. 2005, Montr. Canada, Citeseer, 2005:
592 pp. 1417–1424.

593 [26] J. Pfafferott, Evaluation of earth-to-air heat exchangers with a standardised method to
594 calculate energy efficiency, Energy Build. 35 (2003) 971–983.

595 [27] A. Chel, G.N.Tiwari, Performance evaluation and life cycle cost analysis of earth to air
596 heat exchanger integrated with adobe building for New Delhi composite climate, Energy
597 Build. 41 (2009) 56–66. doi:10.1016/j.enbuild.2008.07.006.

598 [28] D.O. Baxter, Energy exchanges and related temperatures of an earth-tube heat exchanger
599 in the heating mode, Trans. ASAE. 35 (1992) 275–285.

600 [29] P. Hollmuller, B. Lachal, Air–soil heat exchangers for heating and cooling of buildings:
601 Design guidelines, potentials and constraints, system integration and global energy
602 balance, Appl. Energy. 119 (2014) 476–487.

603 [30] X. Li, J. Zhao, Q. Zhou, Inner heat source model with heat and moisture transfer in soil
604 around the underground heat exchanger, Appl. Therm. Eng. 25 (2005) 1565–1577.

605 [31] M. Balghouthi, S. Kooli, A. Farhat, H. Daghari, A. Belghith, Experimental investigation
606 of thermal and moisture behaviors of wet and dry soils with buried capillary heating
607 system, Sol. Energy. 79 (2005) 669–681.

608 [32] R. Kumar, A.R. Sinha, B.K. Singh, U. Modhukalya, A design optimization tool of earth-
609 to-air heat exchanger using a genetic algorithm, Renew. Energy. 33 (2008) 2282–2288.

610 [33] M. Cucumo, S. Cucumo, L. Montoro, A. Vulcano, A one-dimensional transient analytical
611 model for earth-to-air heat exchangers, taking into account condensation phenomena and
612 thermal perturbation from the upper free surface as well as around the buried pipes, Int. J.
613 Heat Mass Transf. 51 (2008) 506–516.

614 [34] G. Gan, Dynamic thermal simulation of horizontal ground heat exchangers for renewable
615 heating and ventilation of buildings, Renew. Energy. 103 (2017) 361–371.

[35] J. Xamán, I. Hernández-Pérez, J. Arce, G. Álvarez, L. Ramírez-Dávila, F. Noh-Pat, Numerical study of earth-to-air heat exchanger: The effect of thermal insulation, Energy Build. 85 (2014) 356–361.

[36] M. Cuny, J. Lin, M. Siroux, V. Magnenet, C. Fond, Influence of coating soil types on the energy of earth-air heat exchanger, Energy Build. 158 (2018) 1000–1012. doi:https://doi.org/10.1016/j.enbuild.2017.10.048.

[37] H. Alkhalaf, M.N. Ibrahim, W. Yan, Numerical Study about Improving the Proficiency of an Earth Air Heat Exchanger System (EAHE) Employing Ground Cover Material, J. Clean Energy Technol. 6 (2018).

[38] G. Gan, Dynamic thermal performance of horizontal ground source heat pumps–The impact of coupled heat and moisture transfer, Energy. 152 (2018) 877–887.

[39] R.T. Muehleisen, Simple design tools for earth-air heat exchangers, Proc. SimBuild. 5 (2012) 723–730.

[40] R. Misra, V. Bansal, G. Das Agrawal, J. Mathur, T. Aseri, Transient analysis based determination of derating factor for earth air tunnel heat exchanger in summer, Energy Build. 58 (2013) 103–110.

[41] V. Bansal, R. Misra, G. Das Agarwal, J. Mathur, 'Derating Factor'new concept for evaluating thermal performance of earth air tunnel heat exchanger: A transient CFD analysis, Appl. Energy. 102 (2013) 418–426.

[42] D.Y. Goswami, A.S. Dhaliwal, Heat transfer analysis in environmental control using an underground air tunnel, J. Sol. Energy Eng. 107 (1985) 141–145.

637 [43] J. Vaz, M.A. Sattler, R. da S. Brum, E.D. dos Santos, L.A. Isoldi, An experimental study
638 on the use of Earth-Air Heat Exchangers (EAHE), Energy Build. 72 (2014) 122–131.

639 [44] T.S. Bisoniya, A. Kumar, P. Baredar, Study on calculation models of earth-air heat
640 exchanger systems, J. Energy. 2014 (2014).

641 [45] S.L. Do, J.-C. Baltazar, J. Haberl, Potential cooling savings from a ground-coupled return-
642 air duct system for residential buildings in hot and humid climates, Energy Build. 103
643 (2015) 206–215.

644 [46] N.M. Thanu, R.L. Sawhney, R.N. Khare, D. Buddhi, An experimental study of the thermal
645 performance of an earth-air-pipe system in single pass mode, Sol. Energy. 71 (2001) 353–
646 364.

647 [47] O. Ozgener, L. Ozgener, Exergoeconomic analysis of an underground air tunnel system
648 for greenhouse cooling system, Int. J. Refrig. 33 (2010) 995–1005.
649 doi:https://doi.org/10.1016/j.ijrefrig.2010.02.008.

650 [48] O. Ozgener, L. Ozgener, Exergetic assessment of EAHEs for building heating in Turkey:
651 A greenhouse case study, Energy Policy. 38 (2010) 5141–5150.
652 doi:https://doi.org/10.1016/j.enpol.2010.04.047.

653 [49] O. Ozgener, L. Ozgener, D.Y. Goswami, Experimental prediction of total thermal
654 resistance of a closed loop EAHE for greenhouse cooling system, Int. Commun. Heat
655 Mass Transf. 38 (2011) 711–716.
656 doi:https://doi.org/10.1016/j.icheatmasstransfer.2011.03.009.

657 [50] O. Ozgener, L. Ozgener, Determining the optimal design of a closed loop earth to air heat

658 exchanger for greenhouse heating by using exergoeconomics, Energy Build. 43 (2011)
659 960–965. doi:https://doi.org/10.1016/j.enbuild.2010.12.020.

660 [51] C.-Y. Hsu, Y.-C. Chiang, Z.-J. Chien, S.-L. Chen, Investigation on performance of
661 building-integrated earth-air heat exchanger, Energy Build. 169 (2018) 444–452.

662 [52] M.S. Uddin, R. Ahmed, M. Rahman, Performance evaluation and life cycle analysis of
663 earth to air heat exchanger in a developing country, Energy Build. 128 (2016) 254–261.

664 [53] J.-U. Lee, T. Kim, S.-B. Leigh, Applications of building-integrated coil-type ground-
665 coupled heat exchangers—Comparison of performances of vertical and horizontal
666 installations, Energy Build. 93 (2015) 99–109.
667 doi:https://doi.org/10.1016/j.enbuild.2015.02.020.

668 [54] Jalaluddin, A. Miyara, K. Tsubaki, S. Inoue, K. Yoshida, Experimental study of several
669 types of ground heat exchanger using a steel pile foundation, Renew. Energy. 36 (2011)
670 764–771. doi:https://doi.org/10.1016/j.renene.2010.08.011.

671 [55] J. Luo, H. Zhao, S. Gui, W. Xiang, J. Rohn, P. Blum, Thermo-economic analysis of four
672 different types of ground heat exchangers in energy piles, Appl. Therm. Eng. 108 (2016)
673 11–19. doi:https://doi.org/10.1016/j.applthermaleng.2016.07.085.

674 [56] M. Benhammou, B. Draoui, M. Zerrouki, Y. Marif, Performance analysis of an earth-to-
675 air heat exchanger assisted by a wind tower for passive cooling of buildings in arid and
676 hot climate, Energy Convers. Manag. 91 (2015) 1–11.

677 [57] M. Kaushal, P. Dhiman, S. Singh, H. Patel, Finite volume and response surface
678 methodology based performance prediction and optimization of a hybrid earth to air

679 tunnel heat exchanger, Energy Build. 104 (2015) 25–35.
680 doi:https://doi.org/10.1016/j.enbuild.2015.07.014.

681 [58] A. Mathur, S. Mathur, G.D. Agrawal, J. Mathur, Comparative study of straight and spiral
682 earth air tunnel heat exchanger system operated in cooling and heating modes, Renew.
683 Energy. 108 (2017) 474–487.

684 [59] M. Maerefat, A.P. Haghighi, Passive cooling of buildings by using integrated earth to air
685 heat exchanger and solar chimney, Renew. Energy. 35 (2010) 2316–2324.

686 [60] H. Li, Y. Yu, F. Niu, M. Shafik, B. Chen, Performance of a coupled cooling system with
687 earth-to-air heat exchanger and solar chimney, Renew. Energy. 62 (2014) 468–477.

688 [61] Y. Yu, H. Li, F. Niu, D. Yu, Investigation of a coupled geothermal cooling system with
689 earth tube and solar chimney, Appl. Energy. 114 (2014) 209–217.
690 doi:https://doi.org/10.1016/j.apenergy.2013.09.038.

691 [62] M.C. Lekhal, R. Belarbi, A.M. Mokhtari, M.-H. Benzaama, R. Bennacer, Thermal
692 performance of a residential house equipped with a combined system: A direct solar floor
693 and an earth–air heat exchanger, Sustain. Cities Soc. (2018).

694 [63] O. Ghasemi-Fare, P. Basu, Influences of ground saturation and thermal boundary
695 condition on energy harvesting using geothermal piles, Energy Build. 165 (2018) 340–
696 351.

697 [64] K.K. Agrawal, R. Misra, T. Yadav, G. Das Agrawal, D.K. Jamuwa, Experimental study to
698 investigate the effect of water impregnation on thermal performance of earth air tunnel
699 heat exchanger for summer cooling in hot and arid climate, Renew. Energy. 120 (2018)

255–265.

[65] F. Niu, Y. Yu, D. Yu, H. Li, Investigation on soil thermal saturation and recovery of an earth to air heat exchanger under different operation strategies, Appl. Therm. Eng. 77 (2015) 90–100.

[66] D. Yang, Y. Guo, J. Zhang, Evaluation of the thermal performance of an earth-to-air heat exchanger (EAHE) in a harmonic thermal environment, Energy Convers. Manag. 109 (2016) 184–194. doi:https://doi.org/10.1016/j.enconman.2015.11.050.

[67] A. Mathur, A. Srivastava, G.D. Agrawal, S. Mathur, J. Mathur, CFD analysis of EATHE system under transient conditions for intermittent operation, Elsevier, 2015.

[68] A. Mathur, A.K. Surana, P. Verma, S. Mathur, G.D. Agrawal, J. Mathur, Investigation of soil thermal saturation and recovery under intermittent and continuous operation of EATHE, Energy Build. 109 (2015) 291–303.

[69] R. Misra, A. Agarwal, V. Bansal, D.K. Jamuwa, NUMERICAL INVESTIGATION OF DYNAMIC INTERACTION OF EARTH AIR TUNNEL HEAT EXCHANGER WITH SURROUNDING SOIL DURING CONTINUOUS AND INTERMITTENT OPERATION IN WINTER, (2017).

[70] A. Agarwal, M.Y. Sheikh, R. Misra, Comparative Study of Transient Conditions for Continuous Operation and Intermittent Operation of EATHE System Operated in Winter Season: A CFD Approach, (2017).

[71] G. Gan, Simulation of dynamic interactions of the earth–air heat exchanger with soil and atmosphere for preheating of ventilation air, Appl. Energy. 158 (2015) 118–132.

[72] A. Mathur, A.K. Surana, S. Mathur, Numerical investigation of the performance and soil temperature recovery of an EATHE system under intermittent operations, Renew. Energy. 95 (2016) 510–521.

[73] Ł. Amanowicz, Influence of geometrical parameters on the flow characteristics of multi-pipe earth-to-air heat exchangers–experimental and CFD investigations, Appl. Energy. 226 (2018) 849–861.

[74] H. Wei, D. Yang, Y. Guo, M. Chen, Coupling of earth-to-air heat exchangers and buoyancy for energy-efficient ventilation of buildings considering dynamic thermal behavior and cooling/heating capacity, Energy. 147 (2018) 587–602.

[75] C.-E. Mehdid, A. Benchabane, A. Rouag, N. Moummi, M.-A. Melhegueg, A. Moummi, M.-L. Benabdi, A. Brima, Thermal design of Earth-to-air heat exchanger. Part II a new transient semi-analytical model and experimental validation for estimating air temperature, J. Clean. Prod. 198 (2018) 1536–1544.

[76] B. Singh, R. Kumar, A.K. Asati, Influence of parameters on performance of earth air heat exchanger in hot-dry climate, J. Mech. Sci. Technol. 32 (2018) 5457–5463.

[77] M. Habibi, A. Hakkaki-Fard, Evaluation and improvement of the thermal performance of different types of horizontal ground heat exchangers based on techno-economic analysis, Energy Convers. Manag. 171 (2018) 1177–1192.

[78] Y. Noorollahi, R. Saeidi, M. Mohammadi, A. Amiri, M. Hosseinzadeh, The effects of ground heat exchanger parameters changes on geothermal heat pump performance–A review, Appl. Therm. Eng. 129 (2018) 1645–1658.

[79] N. Barsoum, H. Yong, H. Chang, Modeling and Cost Effective Simulation of Stand Alone Solar and Micro-Hydro Energy, in: Andhra Univ. AU Coll. Eng. Visakapatnam, India, IEEE Hyderabad Section, 2008: pp. 809–814.

[80] P. Ekins, S. Speck, Environmental tax reform (ETR): a policy for green growth, Oxford University Press, 2011. https://books.google.com/books?hl=en&lr=&id=izAGyP7g4OoC&oi=fnd&pg=PP2&dq=Ekins+P,+Speck+S,+editors.+Environmental+tax+reform+(ETR):+a+policy+for+green+growth.+Oxford%3B+New+York:+Oxford+University+Press&ots=qtlNiuPGgT&sig=-RDnAzVDHhPQWY9_kfg9pFKIemo#v=on.

[81] W.J. Baumol, On Taxation and the Control of Externalities, Am. Econ. Rev. 62 (1972) 307–322. http://www.jstor.org/stable/1803378.

[82] W.J. Baumol, W.E. Oates, The Use of Standards and Prices for Protection of the Environment BT - The Economics of Environment: Papers from Four Nations, in: P. Bohm, A. V Kneese (Eds.), Palgrave Macmillan UK, London, 1971: pp. 53–65. doi:10.1007/978-1-349-01379-1_4.

[83] High Energy Consumption Patterns Jeopardizing Iran’s Development Plans | Financial Tribune, (n.d.). https://financialtribune.com/articles/energy/56356/high-energy-consumption-patterns-jeopardizing-irans-development-plans.

[84] Renewable Energy and Energy Efficiency Organization, (n.d.). http://www.satba.gov.ir/en/home.

[85] Wind energy. Renewable energy. BP Statistical Review of World Energy. Energy

763 economics, (n.d.). https://www.bp.com/en/global/corporate/energy-economics/statistical-
764 review-of-world-energy/renewable-energy/wind-energy.html.

765 [86] I.R.OF IRAN Meteorological Organization ::, (n.d.). http://irimo.ir/eng/index.php.

766 [87] J.F. Wendt, Computational fluid dynamics: an introduction, Springer Science & Business
767 Media, 2008.

768 [88] M. De Paepe, A. Janssens, Thermo-hydraulic design of earth-air heat exchangers, Energy
769 Build. 35 (2003) 389–397.

770 [89] Vent-Axia Ventilation Design Guidelines, (n.d.). https://www.vent-
771 axia.com/sites/default/files/Ventilation Design Guidelines 2.pdf.

772 [90] A. Artur, J.R. Bell, W.L. Angel, HVAC Equations, Data, and Rules of Thumb, (2015).

773 [91] M.H. Ashourian, S.M. Cherati, A.A. Mohd Zin, N. Niknam, A.S. Mokhtar, M. Anwari,
774 Optimal green energy management for island resorts in Malaysia, Renew. Energy. 51
775 (2013) 36–45. doi:10.1016/J.RENENE.2012.08.056.

776 [92] HOMER - Hybrid Renewable and Distributed Generation System Design Software, (n.d.).
777 https://www.homerenergy.com/.

778 [93] S. Bahramara, M.P. Moghaddam, M.R. Haghifam, Optimal planning of hybrid renewable
779 energy systems using HOMER: A review, Renew. Sustain. Energy Rev. 62 (2016) 609–
780 620. doi:10.1016/J.RSER.2016.05.039.

781 [94] K.K. Shah, A.S. Mundada, J.M. Pearce, Performance of U.S. hybrid distributed energy
782 systems: Solar photovoltaic, battery and combined heat and power, Energy Convers.

783 Manag. 105 (2015) 71–80. doi:10.1016/J.ENCONMAN.2015.07.048.

784 [95] A. Nosrat, J.M. Pearce, Dispatch strategy and model for hybrid photovoltaic and
785 trigeneration power systems, Appl. Energy. 88 (2011) 3270–3276.
786 doi:10.1016/J.APENERGY.2011.02.044.

787 [96] A. Al-Sharafi, A.Z. Sahin, B.S. Yilbas, Overall performance index for hybrid power
788 plants, Energy Convers. Manag. 100 (2015) 103–116.
789 doi:10.1016/J.ENCONMAN.2015.04.067.

790 [97] M.S. Islam, A techno-economic feasibility analysis of hybrid renewable energy supply
791 options for a grid-connected large office building in southeastern part of France, Sustain.
792 Cities Soc. 38 (2018) 492–508. doi:10.1016/J.SCS.2018.01.022.

793 [98] L.M. Halabi, S. Mekhilef, L. Olatomiwa, J. Hazelton, Performance analysis of hybrid
794 PV/diesel/battery system using HOMER: A case study Sabah, Malaysia, Energy Convers.
795 Manag. 144 (2017) 322–339. doi:10.1016/j.enconman.2017.04.070.

796 [99] M. Baneshi, F. Hadianfard, Techno-economic feasibility of hybrid diesel/PV/wind/battery
797 electricity generation systems for non-residential large electricity consumers under
798 southern Iran climate conditions, Energy Convers. Manag. 127 (2016) 233–244.
799 doi:10.1016/j.enconman.2016.09.008.

800 [100] Eocycle's small wind turbines, (n.d.). https://eocycle.com/small-wind-turbine/.

801 [101] CELLCUBE® FB 30-130, (n.d.). https://www.vsunenergy.com.au/wp-
802 content/uploads/2017/02/Environmental-Controls.pdf.

803 [102] O. Aalde, Hybrid renewable-diesel energy systems in an off-grid arctic community of

804 Svalbard, (n.d.).

805 [103] Electric boilers » Varmeteknikk AS - Miljøvennlig oppvarming med elektrokjeler, (n.d.).
806 http://www.varmeteknikk.no/low-voltage-boilers.

807 [104] A. Πέτρου, A. Petrou, Operational Optimization of the Geothermal Power Plant
808 Unterhaching, (2015).

809 [105] A.J. Marszal, P. Heiselberg, Life cycle cost analysis of a multi-storey residential net zero
810 energy building in Denmark, Energy. 36 (2011) 5600–5609.

811 [106] M. Hossain, S. Mekhilef, L. Olatomiwa, Performance evaluation of a stand-alone PV-
812 wind-diesel-battery hybrid system feasible for a large resort center in South China Sea,
813 Malaysia, Sustain. Cities Soc. 28 (2017) 358–366. doi:10.1016/J.SCS.2016.10.008.

814 [107] Hydrogen Generator, (n.d.). https://www.fuelcellstore.com/hydrogen-
815 equipment/hydrogen-production-electrolyzers/ql-1000-hydrogen-generator.

816 [108] S.C. Bhattacharyya, Energy economics: concepts, issues, markets and governance,
817 Springer Science & Business Media, 2011.

818 [109] G.J. Dalton, D.A. Lockington, T.E. Baldock, Feasibility analysis of renewable energy
819 supply options for a grid-connected large hotel, Renew. Energy. 34 (2009) 955–964.

820 [110] 7.133 Renewable Fraction, (n.d.).
821 https://www.homerenergy.com/products/pro/docs/3.11/_renewable_fraction.html.

822 [111] A.R. Alghannam, O. Investigations of Performance of Earth Tube Heat Exchanger of
823 Sandy Soil in Hot Arid Climate, J. Appl. Sci. Res. 8 (2012) 3044–3052.

[112] W. Morshed, L. Leso, L. Conti, G. Rossi, S. Simonini, M. Barbari, Cooling performance of earth-to-air heat exchangers applied to a poultry barn in semi-desert areas of south Iraq, Int. J. Agric. Biol. Eng. 11 (2018) 47–53.